International Journal of Air-Conditioning and Refrigeration Vol. 15, No. 4 (2007) 156~162

# Flow Efficiency in Multi-Louvered Fins Having Large Louver-to-Fin Pitch Ratio

Nae Hyun Kim*, Jin Pyo Cho, Do Young Kim, Hyun Jin Kim

*Department of Mechanical Engineering, University of Incheon, Incheon 402-749, Korea*

(Received August 6, 2007; Revision received October 30, 2007)

**Abstract**

Flow visualization experiments were conducted for two louver arrays having large louver pitch ratio ($L_p/F_p$ = 1.0 and 1.4). Flow efficiencies and critical Reynolds numbers were obtained from the data, and were compared with existing correlations. The correlations failed to predict the present flow efficiency data adequately; some correlation overpredicted the data, while others underpredicted the data. Large louver pitch ratio of the present model, which is outside of the applicable range of the correlations may partly be responsible. The critical Reynolds numbers obtained from the present flow visualization data were in close agreement with those obtained from the heat transfer tests on actual flat tube heat exchangers. Existing correlations on the critical Reynolds number generally overpredicted the present data.

*Key words*: Flow visualization; Flow efficiency; Brazed aluminum heat exchanger; Flat tube; Louver fin

## Nomenclature

$c_p$ : sepcific heat [J kg$^{-1}$ s$^{-1}$]
$D$ : ideal transverse distance [m]
$F_p$ : fin pitch [m]
$f$ : airside friction factor (dimensionless)
$h$ : heat transfer coefficient [W m$^{-2}$ K$^{-1}$]
j : Colburn j factor (dimensionless), $\left(=\frac{h}{\rho V_{\max} c_p}\right)$
$L$ : louver depth [m]
$L_p$ : louver pitch [m]
$N$ : actual transverse distance (dimensionless)
$Re_c$ : critical Reynolds number (dimensionless)
$Re_L$ : Reynolds number based on $L_p$ (dimensionless), $\left(=\frac{V_{\max} L_p}{\nu}\right)$
$S$ : non-louvered inlet and exit fin length [m]
$t$ : fin thickness [m]
$V_{\max}$ : velocity based on the minimum flow area of the frontal surface [ms-1]

### *Greek Symbols*

$\alpha$ : louver angle [deg]
$\beta$ : flow angle [deg]
$\eta$ : flow efficiency (dimensionless)
$\eta_{\max}$ : asymptotic flow efficiency (dimensionless)
$\rho$ : density [kg m$^{-3}$]
$\nu$ : kinematic viscosity [m$^2$ s$^{-1}$]

## 1. Introduction

Fin-and-tube heat exchangers have been widely used as condensers or evaporators in a household air-conditioning system. In the forced convective heat transfer between air and refrigerant, the controlling thermal resistance is on the air-side. To improve the air-side performance, rigorous efforts have been made, which include a usage of high performance fins, and of small diameter tubes, etc. However, fin-and-tube heat exchangers have inherent short-comings such as the contact resistance between fins and tubes, the existence of a low performance region behind tubes, etc. These short-comings may be overcome if fins and tubes are soldered, and low profile flat tubes with high performance fins are used. Brazed aluminum flat-tube heat exchangers with louver fins could be

*Corresponding author. Tel.: +82-32-770-8420, Fax: +82-32-770-8410
E-mail address: knh0001@incheon.ac.kr

the choice. Flat tube heat exchangers have been used as condensers of automotive air conditioning units for more than ten years, and they are replacing fin-and-tube condensers of residential air-conditioning units. The possibility of replacing the residential fin-and-tube heat exchangers by flat tube heat exchangers has been studied by Webb and Jung[1]. They showed that, for the same air-side thermal capacity, the flat-tube geometry requires less than half the heat exchanger volume compared with the fin-and-tube counterpart. The advantage of flat-tube heat exchangers has further been studied by Webb and Lee[2]. They compared the thermal performance of flat tube condenser having 866 fins per meter with that of the fin-and-tube condenser having 7.0 mm round tubes and 1024 fins per meter. The flat tube condenser was shown to reduce the material up to 50%. One major challenge for application of the flat tube condenser to a residential air-conditioner is to deal with the reduced frontal air velocity. The frontal air velocity of the residential system is much lower (0.5 m/s ~ 1.5 m/s) than that of the automotive system (2 m/s ~ 5 m/s), where most of the flat tube heat exchanger technology is based. The thermal performance of the louver fin is known to decrease significantly as the flow velocity decreases.

Although louvered surfaces have been used since the 1950s, the flow characteristics have not been unveiled until the pioneering work by Davenport[3]. He showed that, through flow visualization study, the flow did not pass through the louvers at low Reynolds numbers. At high Reynolds numbers, however, the flow became nearly parallel to the louvers. He speculated that, at low air velocities, the developing boundary layers on adjacent louvers became thick enough to effectively block the passage, resulting in nearly axial flow through the array. Achaichia and Cowell[4] further confirmed that, through heat transfer tests on flat tube heat exchangers having louvered plate fins, the heat transfer coefficients were close to those of the laminar boundary layer for a flat plate at high Reynolds numbers. At sufficiently low Reynolds numbers, however, the heat transfer coefficients approached those of the duct flow, resulting significant decrease in the heat transfer coefficient. Two types of flow were identified within the louvered plate fin array; duct-directed flow and louver-directed flow. The amount of either flow depended on the louver geometry such as fin pitch, louver pitch, louver angle as well as the Reynolds number. The louver- or duct-directed flow is illustrated in Fig. 1. The above discussions reveal that the flow direction has a profound effect on the thermal performance of the louver fin. It is particularly crucial for low Reynolds number application, where both duct- and louver-directed flow prevails.

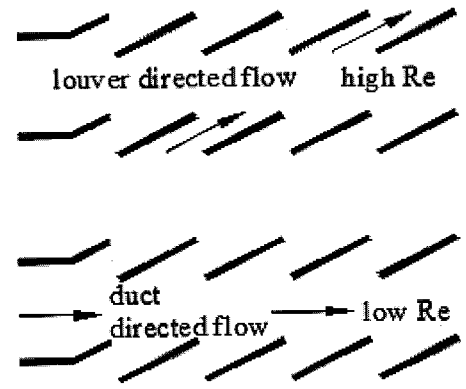


Fig. 1. Flow structure along louvers.

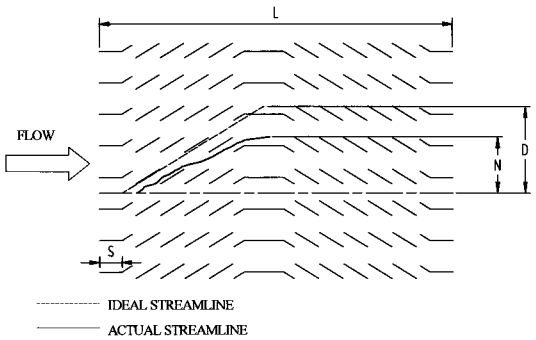


Fig. 2. Definition of flow efficiency.

To describe the flow direction in a louver fin, "flow efficiency ( $\eta$ )" has been used, which implies the ratio of the louver-directed flow to the total flow. A 100% efficiency represents ideal louver-directed flow, while 0% represents complete duct-directed flow. The literature shows that two different definitions of flow efficiency exist. In flow visualization studies using dye injection[5,6], the flow efficiency is defined as the ratio of actual transverse distance (N) traveled by the dye to the ideal distance (D) if the flow were aligned with the louver. The flow efficiency is illustrated in Fig. 2.

$$\eta = \frac{N}{D} \tag{1}$$

Another definitions is from numerical simulations[7,8], where the flow angle can be easily obtained

for individual louvers. The flow efficiency is defined as the ratio of the mean flow angle ( $\beta$ ), which is obtained by averaging flow angles throughout the louver array to louver angle ( $\alpha$ ).

$$\eta = \frac{\beta}{\alpha} \tag{2}$$

The literature reveals four flow efficiency correlations. Webb and Trauger[5] conducted flow visualization experiments using models having 5 spanwise louver arrays, for $0.49 \leq L_p/F_p \leq 1.31$ and two louver angles (20° and 30°). Reynolds number ($Re_L$) ranged from 400 to 4000. Their results showed that, above a critical Reynolds number ($Re_c$), the flow efficiency was only affected by the louver pitch ratio.

$$Re_c = 828\left(\frac{\alpha}{90}\right)^{-0.34} \tag{3}$$

$$\eta = 0.95\left(\frac{L_p}{F_p}\right)^{0.23} \tag{4}$$

Significant drop of flow efficiency was noted below the critical Reynolds number. The flow efficiency increased with the Reynolds number, louver angle and louver pitch ratio until a critical Reynolds number is reached.

$$\eta = 0.091 Re_L^{0.39}\left(\frac{L_p}{F_p}\right)^{0.44}\left(\frac{\alpha}{90}\right)^{0.3} \tag{5}$$

It is interesting to note that, in Webb and Trauger[5] correlation, the critical Reynolds number depends only on the louver angle, while the flow efficiency beyond the critical Reynolds number depends only on the louver pitch ratio.

Another flow efficiency correlation was proposed by Bellows[6] from flow visualization experiments. His correlation is based on three samples having $0.45 \leq L_p/F_p \leq 0.92$ and $18° \leq \alpha$ 28°. The samples had 13 spanwise louver arrays. The general correlation was developed as

$$\eta = \left[-5 - 300/Re_L - 10\left(\frac{F_p}{L_p}\right) + 1.34\alpha\right]/\alpha \tag{6}$$

The critical Reynolds number was obtained from $\eta/\eta_{max} = 0.95$ as

$$Re_c = \frac{600}{[-5 - 10(F_p/L_p) + 1.34\alpha]} \tag{7}$$

Achaichia and Cowell[7] numerically calculated the flow through a simplified two-dimensional louver array for $0.4 \leq L_p/F_p \leq 1.0$ and $15° \leq \alpha \leq 35°$. The louvers were assumed to be infinitely thin, and the flow was assumed to be fully developed. From the numerical results, the following flow efficiency correlation was obtained.

$$\eta = \left[0.936 - 243/Re_L - 1.76\left(\frac{F_p}{L_p}\right) + 0.995\alpha\right]/\alpha \tag{8}$$

The critical Reynolds number was obtained from $\eta/\eta_{max} = 0.95$ as

$$Re_c = \frac{4860}{[0.936 - 1.76(F_p/L_p) + 0.995\alpha]} \tag{9}$$

Zhang and Tafti[8] improved the Achaichia and Cowell's[7] numerical calculation by considering full louver array and fin thickness. The proposed flow efficiency correlation is

$$\eta = \eta_1 + \eta_2 + \eta_3 \tag{10}$$

$$\eta_1 = \frac{d^{0.5}}{d^{0.5} + 1/\sqrt{\cos\alpha}} \tag{11}$$

$$\eta_2 = \frac{0.357}{(F_p/L_p)(t/L_p)}\left(\frac{30}{\alpha}\right)^{(F_p - 0.9)} \tag{12}$$

$$\eta_3 = \frac{70(t/L_p)}{\left[\frac{Re_L(F_p - t)}{F_p}\right]^{[(0.38/F_p/L_p)^{1.1} + 0.02\alpha]}} \tag{13}$$

$$d = \frac{\sin\alpha - t/L_p}{F_p/L_p - \sin\alpha - (t/L_p)\cos\alpha} \tag{14}$$

The above correlation is applicable for $0.5 \leq L_p/F_p \leq 1.26$ and $15° \leq \alpha \leq 50°$, $0.05 \leq t/L_p \leq 0.2$ and $0.1 \leq d \leq 1.9$.

As noted earlier, the flat tube heat exchanger has been used mainly for an automotive system, where the flow velocity is rather high. For a household air-conditioner, the frontal air velocity is between 0.5 m/s

and 1.5 m/s with corresponding Reynolds number ($Re_L$) between 35 and 120 (for 1.0 mm louver pitch). It has been revealed by many investigators that, as the Reynolds number decreases, more flow tends to be duct-oriented, which significantly decreases the heat transfer coefficient. This situation may be remedied if the fin pitch is decreased or louver pitch is increased. Smaller the fin pinch (or lager the louver pitch), more flow is expected to follow the louver. In search for a suitable louver geometry for a household application, Cho et al.[9] tested 12 flat aluminum heat exchangers having small fin pitches and large louver pitch ($L_p$ = 1.7 mm and $1.2 \leq L_p/F_p \leq 1.6$). The critical Reynolds numbers were obtained from the heat transfer data (corresponding to the peak of the j factor curve). The critical Reynolds numbers were significantly lower than the predictions by Webb and Trauger[5], which suggests more flow visualization study is needed, especially for a large louver pitch ratio ($L_p/F_p$) range. The literature shows very limited data for $L_p/F_p \geq 1.0$.

In the present study, flow visualization experiments were conducted for two louver arrays having $L_p/F_p$ = 1.0 and 1.4. Critical Reynolds numbers as well as flow efficiencies were obtained from the data, and compared with existing correlations. Tests were conducted in a water tunnel for $50 \leq Re_L \leq 400$.

## 2. Experiment

### *2.1 Louver array samples*

Flow visualization experiments were conducted in a water tunnel. In order to simulate the actual louver array using large scale models, both geometric and dynamic similarity should be satisfied. The present models were made to simulate the louver arrays of flat tube heat exchangers tested by Cho et al.[9]. The geometric dimensions and the sketch of the models are shown in Fig. 3. The louver angle is 27 oC, and the louver pitch is 7.0 mm. Considering that the louver pitch of the samples tested by Cho et al.[9] was 1.7 mm, the present model was enlarged 4.1 times. Two different fin pitches (7.0 mm and 5.0 mm) were selected, which yielded $L_p/F_p$ = 1.0 and 1.4. The test section was a rectangular channel (5 mm x 98 mm x 300 mm for $L_p/F_p$ = 1.0 and 5 mm x 70 mm x 300 mm for $L_p/F_p$ = 1.4) made from 5.0 mm thick acryl plates. At the top and bottom plates, near the end of the channel, grooves were machined for insertion of the louver elements. The louver elements were made from 0.64 mm thick brass sheet, and were 7.0 mm high. The louver array consisted of 13 spanwise rows of louver elements.

### *2.2 Experimental apparatus and test procedures*

The flow visualization tests were conducted in a specially made water tunnel. A schematic drawing of the test setup is shown in Fig. 4. The test section was connected to the upper and lower reservoirs, which were made from acryl plates. The size of the upper reservoir was 2 m x 2 m x 1 m, and that of the lower reservoir was 0.5 m x 0.5 m x 0.5 m. A flow control valve was mounted at downstream of the lower reservoir. The flow rate was measured by weighing the drained water. Flow visualization was performed using a dye injection technique. The dye was a powder (Fuchsine Basic), which was mixed with water. The color of the solution was deep red, and the density was approximately the same as that of water. Dye was injected into the flow using a hypodermic needle, which was connected to a dye reservoir by plastic tubing. The dye reservoir was mounted 1 m above the channel test section, which allowed gravity flow of the dye. The injection rate of the dye was controlled by a control valve placed on the tubing. The visualization tests were conducted as follows.

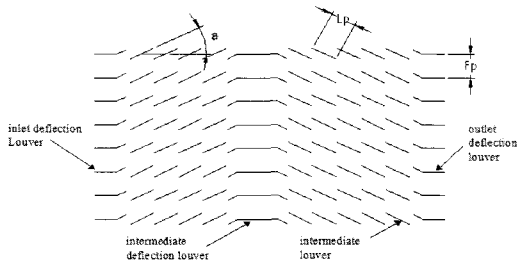


Fig. 3. Sketch of the louver array

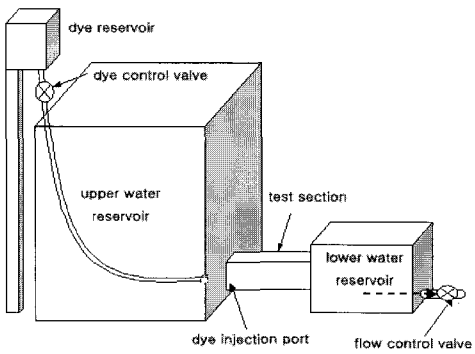


Fig. 4. Schematic configuration of water tunnel.

(1) Fill up both upper and lower reservoir with water.
(2) Set the flow rate at the lowest value using the flow control valve.
(3) Introduce the dye and record the flow using a camera.
(4) Increase the flow rate and repeat (1) to (3)

Although the upper reservoir had a large cross-sectional area (2 m x 2 m), the water height in the upper reservoir decreased during the experiment. The decrease during one test (conducted within one minute) was approximately 6 mm at $Re_L$ = 50, and 60 mm $Re_L$ = 500. The corresponding change of velocity was 0.2% at $Re_L$ = 50, and 2 % at $Re_L$ = 500. No attempt was made to maintain the water level in the upper reservoir uniform by adding a flesh water into the reservoir. We were concerned that the added water might disturb the flow into the test channel.

Data reduction was a simple procedure. The data were quantified as a flow efficiency vs. Reynolds number ($Re_L$). Flow efficiency was determined from the photo taken during the test, following the definition of Eq. (1), and Reynolds number ($Re_L$) was determined by measuring the drained water.

## 3. Results and discussion

Data were taken for two louver samples over a Reynolds number of 50 < $Re_L$ < 400. Typical flow visualization photos are shown in Fig. 5 for $L_p/F_p$ = 1.4. At two extreme Reynolds numbers ($Re_L$ = 60 and 359), streak lines are clearly seen without any blur caused by unsteadiness of the flow, suggesting that the flow is laminar. The injected dye travels down along the louver to the center of the array, and then deflected up due to the deflection louver, travels up along the louver, and exits the array. At $Re_L$ = 60, the spanwise travel distance form the inlet to the center of the array is approximately four louver pitch. This distance increases to approxiamtely five at $Re_L$ = 359.

The flow efficiency was calculated using Eq. (1), and the results are plotted in Fig. 6 for $L_p/F_p$ = 1.4. This figure shows that the flow efficiency is 0.91 at $Re_L$ = 359, slightly decreases to 0.85 at $Re_L$ = 91, and then significantly decreases afterwards. Predictions by four existing flow efficiency correlations are also shown in the figure. Achaichia and Cowell[7], Bellows[6] and Zhang and Tafti[8] correlation generally predict the trend of the data, with slight overprediction by Achaichia and Cowell[7], and underprediction by Bellows[6] and Zhang and Tafti[8]. As noted

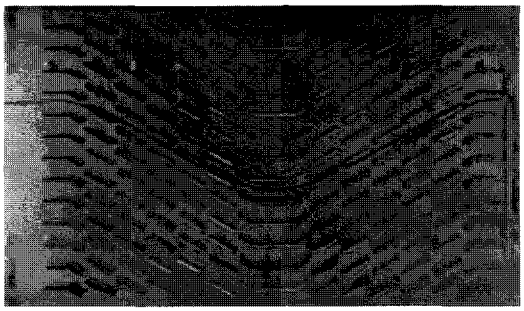

(a) $Re_L$ = 60

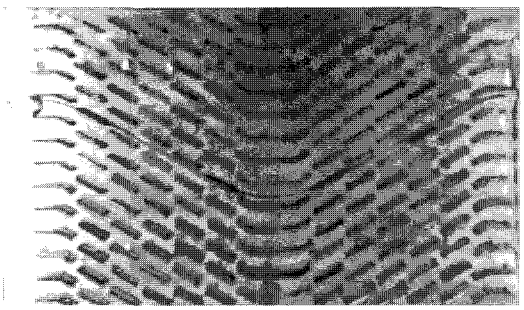

(b) $Re_L$ = 359

Fig. 5. Steak Line in the louver fin ($L_p/F_p$ = 1.4)

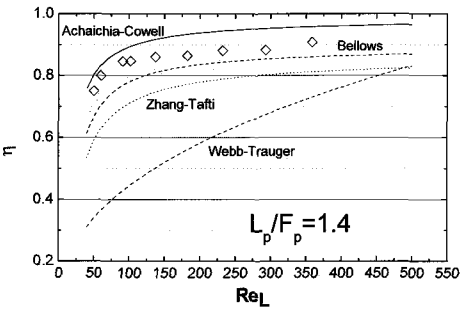


Fig. 6. Flow efficiency for $L_p/F_p$ = 1.4

earlier, Achaichia and Cowell[7] assumed an infinitely thin louver and fully developed flow, which usually causes an overprediction of the flow efficiency. The Bellows[6] correlation was developed from experimental data with 0.45 ≤ $L_p/F_p$ ≤ 0.92, which is smaller than the present louver pitch ratio $L_p/F_p$ = 1.4. Same argument may apply to Zhang and Tafti[8], who developed a correlation from numerical data with 0.5 ≤ $L_p/F_p$ ≤ 1.26. Fig. 6 shows that Webb and Trauger[5] correlation significantly underpredict the data. The reason may be attributed to the small number of louver rows of Webb and Trauger's samples. Their samples consisted of five rows of louvers. Recent

study by Springer and Thole[10] and Beamer et al.[11] revealed that, as fewer rows of louvers are used, the flow is forced to become duct-directed because of the end-wall effects. Duct-directed flow will lower the flow efficiency. Springer and Thole[10] recommended samples of more than 19 rows for a proper flow visualization test. The $L_p/F_p$ = 1.0 data are shown in Fig. 7. The flow efficiency is 0.83 at $Re_L$ = 224, decreases to 0.79 at $Re_L$ = 98, and then significantly decreases afterwards. The predictions show similar trend as $L_p/F_p$ = 1.4 ; slight overprediction by Achaichia and Cowell[7], underprediction by Bellows[6] and Zhang and Tafti[8], and significant underprediction by Webb and Trauger[5].

The flow efficiency data generally show a sudden drop below a certain Reynolds number (critical Reynolds number). There exist two different definitions on critical Reynolds number. Webb and Trauger[5] noted that above a certain Reynolds number, the flow efficiency is constant, independent of the Reynolds number. He proposed a correlation for the critical Reynolds number [Eq. (3)]. Another definition was proposed by Achaichia and Cowell[7]. The critical Reynolds number is defined as the one, where the flow efficiency is 95% of the asymptotic value. They proposed a correlation from the numerical study [Eq. (9)]. Bellows[6] also proposed a correlation following the definition of Achaichia and Cowell[7] [Eq. (7)]. Fig. 8 shows the present flow efficiency data plotted in the same figure. As the Reynolds number decreases, the flow efficiency slightly decreases up to a certain Reynolds number, and then significantly decreases afterwards. In the present study, the Reynolds number, where a sudden drop of flow efficiency occurs is defined as a critical Reynolds number. This definition is in line with that of Webb and Trauger[5], although the flow efficiency slightly increases above the critical Reynolds number. The Achaichia and Cowell[7] definition is not possible in the present study, because the asymptotic flow efficiency data are not available.

Table 1 shows the present critical Reynolds number compared with predictions by the correlations. Achiachia and Cowell[7] and Bellows[6] predictions slightly overpredict the data. The small $L_p/F_p$ ratio of Achiachia and Cowell[7] and Bellows[6] may partly be responsible. Table 1 shows that Webb and Trauger[5] correlation significantly overpredicts the data. The significant overprediction is probably due to the deficiency in their flow visualization models as discussed previously.

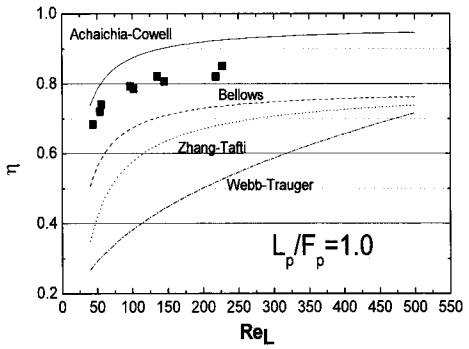


Fig. 7. Flow efficiency for $L_p/F_p$ = 1.0

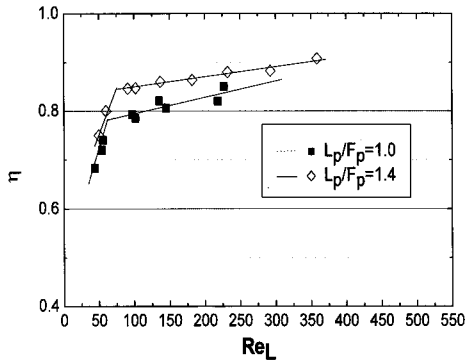


Fig. 8. Flow efficiency of the present study

Cho et al.[9] tested flat aluminum heat exchangers having the same louver configuration as the present study ($L_p$ = 1.7 mm and 1.2 ≤ $L_p/F_p$ ≤ 1.6). Fig. 9 show the j and f factors for the three samples. As the Reynolds number decreases, the j factor increases. Below a certain Reynolds number (critical Reynolds number), however, the j factor decreases as the Reynolds number decreases, yielding a peak in the j factor curve. The critical Reynolds numbers were obtained from Fig. 9, and are listed in Table 1. Table 1 reveals that the critical Reynolds numbers obtained from the heat transfer tests are in close agreement with those obtained from the flow visualization tests. One thing to notice is that both critical Reynolds numbers increase as the louver pitch ratio increases. The critical Reynolds numbers obtained from Achaicha and Cowell[7] and Bellows[6] correlation decrease as the louver pitch ratio increases, and those from Webb and Trauger[5] correlation are independent of the louver pitch ratio. This suggests that extrapolation of the existing critical Reynolds correlations outside the recommended range should be made with caution.

Table 1. Critical Reynolds numbers

| Investigators | $L_p/F_p$ | | |
|---|---|---|---|
| | 1.0 | 1.2 | 1.4 |
| Present flow visualization data | $\simeq 60$ | | $\simeq 75$ |
| Heat transfer data[9] | | $\simeq 70$ | $\simeq 100$ |
| Webb & Trauger[5] | 1246 | 1246 | 1246 |
| Achaichia & Cowell[7] | 184 | 183 | 182 |
| Bellows[6] | 261 | 249 | 237 |

## 4. Conclusions

In this study, flow visualization experiments were conducted for two louver arrays having large louver pitch ratio ($L_p/F_p$ = 1.0 and 1.4). Flow efficiencies and critical Reynolds numbers were obtained from the data, and were compared with the existing correlations. Listed below are major findings.

1) Existing correlations fail to predict the present flow efficiency data adequately. Some correlation overpredicts the data, while others underpredict the data. Large louver pitch ratio of the present model, which is outside of the applicable range of the correlations may partly be responsible.
2) Existing correlations on the critical Reynolds number generally overpredict the critical Reynolds number of the present study. Again, large louver pitch ratio of the present model may partly be responsible.
3) The critical Reynolds numbers obtained from the present flow visualization study are in close agreement with those obtained from the heat transfer tests on actual flat tube heat exchangers.
4) For the range of Reynolds number of the present study ($50 \leq Re_L \leq 400$), the streak line was clear without any blur, suggesting steady laminar flow.

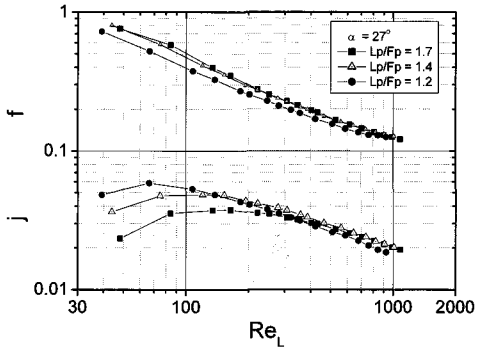


Fig. 9. j and f factors of the flat tube heat exchangers tested by Cho et al.[9]

## References

[1] Webb, R. L. and Jung, S. H., 1992, Air-side performance of enhanced brazed aluminum heat exchangers, ASHRAE Trans., Vol 98, No. 2, pp. 391-410.

[2] Webb, R. L. and Lee, H., 2001, Brazed aluminum heat exchangers for residential air-conditioning, J. Enhanced Heat Transfer, Vol 8, pp. 1-14.

[3] Davernport, C. J., 1980, Heat transfer and fluid flow in louvered triangular ducts, Ph.D. Thesis, Lanchester Polytechnic, U. K.

[4] Achaichia A. and Cowell, T. A., 1988, Heat transfer and pressure drop characteristics of flat tube and louvered plate fin surfaces, Exp. Thermal Fluid Science, Vol 1, pp. 147-157.

[5] Webb R. L. and Trauger, P. E., 1991, Flow structure in the louvered fin heat exchanger geometry, Exp. Thermal Fluid Science, Vol 4, pp. 205-217.

[6] Bellows, K. D., 1997, Flow visualization of louvered fin heat exchangers, M.S. Thesis, University of Ilinois at Urbana Champaign, IL.

[7] Achaichia A and Cowell, T. A., 1988, A finite difference analysis of fully developed periodic laminar flow in inclined louvered arrays, in Proceedings of Second UK National Heat Transfer Conference, Glassgow, pp. 883-888.

[8] Zhang, X. and Tafti, D. K., 2003, Flow efficiency in multi-louvered fins, Int. J. Heat Mass Transfer, Vol. 46, pp. 1737-1750.

[9] Cho, J. P., Oh, W. K., Kim, N. H. and Youn, B., 2002, Air-side performance of louver-finned flat aluminum heat exchanges at a low velocity region, KSME J. Vol. 26, No. 12, pp. 1681-1691.

[10] Springer M. E., Thole, K. A., 1998, Experimental design for flow field studies of louvered fins, Exp. Thermal Fluid Science, Vol 18, pp. 258-269.

[11] Beamer, H. E., Ghosh, D., Bellows, K. D., Huang, L. J., Jacobi, A. M., 1998. Applied CFD and experiment for automotive compact heat exchanger development, SAE 980426.